We are IntechOpen, the world's leading publisher of Open Access books
Built by scientists, for scientists

6,900
Open access books available

186,000
International authors and editors

200M
Downloads

Our authors are among the

154
Countries delivered to

TOP 1%
most cited scientists

12.2%
Contributors from top 500 universities

CLARIVATE ANALYTICS
BOOK CITATION INDEX
INDEXED

WEB OF SCIENCE™

Selection of our books indexed in the Book Citation Index
in Web of Science™ Core Collection (BKCI)

Interested in publishing with us?
Contact book.department@intechopen.com

Numbers displayed above are based on latest data collected.
For more information visit www.intechopen.com

Chapter

CFD Optimization Method to Design Foam Residue Traps for Full Mold Casting

Yuto Takagi, Masahiro Inagaki and Ken'ichi Yano

Abstract

Full mold casting is a casting process in which a mold made of wood or metal is substituted for a styrofoam model. This metal casting process is advantageous for the production of large-sized castings because it uses a foamed model. However, this unique process of melting a foamed model causes a problem which is the foamed model remains dissolved in the casting. This is called foam residue defect and is specific to full mold casting. In this study, we propose a new casting design called a residue trap to reduce these residue defects. This residue trap collects the residue of foam models included in the molten metal, which tends to be generated when the temperature of the molten metal becomes low by being attached to the product part in the same way to overflows. We also optimized the shape of the residue trap in terms of easing of post-treatment and increasing efficiency of collecting foam residue. Eventually, the effectiveness of the residue trap was verified by actual full mold casting experiments.

Keywords: full mold casting, foam residue, CFD simulation, shape optimization, genetic algorithm

1. Introduction

Unlike conventional sand-casting using wooden molds, full mold casting offers the advantage of near-net shaping without the need for a draft angle in the product shape. As a result, the number of person-hours in post-casting processing can be decreased, reducing cost and shortening delivery times. However, the occurrence of residue defects, which is a phenomenon unique to the full mold casting method, is a major problem in the manufacture of large castings by this method. This is a serious issue that significantly impairs the quality of the product because the unresolved part of the foam model is mixed in with the product.

As a measure against defects in residue at the casting site, the pouring temperature can be increased to facilitate the thermal decomposition of a foam model. However, due to the high temperature inside the product, the volume shrinkage due to solidification increases and shrinkage nests tend to occur. On the other hand, if the pouring temperature is lowered to prevent shrinkage cavity, the foam model cannot be thermally decomposed efficiently and residue defects are generated. Although there is also a method of installing multiple gates, which are the inlets to the product, to improve the molten metal turnover, a flow of metal that rolls in the foam model is generated, and residue defects are more likely to occur.

Traditionally, these casting conditions and schemes have been determined based on the experience and intuition of skilled workers. In recent years, however, the use of computational fluid dynamics (CFD)-based simulations has made it possible to study appropriate conditions and solutions in advance based on the analytical results of the melt flow and solidification processes, thereby reducing the cost and time required for trial manufacture and experimentation. Particularly, solidification simulations are used to study casting conditions and solutions for shrinkage cavity defects, which can be estimated with high accuracy by comparison and verification with experiments [1]. The authors have also been optimizing the shapes of the runners in die castings by using CFD simulation and the shape optimization method for molten metal flow [2].

In recent years, the full mold casting method and the vanishing model casting method have been actively researched. Maruyama et al. have collected, analyzed, and investigated the pyrolysis products generated during the filling of molten metal in the vanishing model casting process [3]. Koroyasu et al. reported on the adiabatic properties of a coating in the vanishing model casting method and conducted a simple simulation of molten aluminum alloy flow in that method to investigate the influence of the air permeability of the coating, the presence or absence of depressurization, and casting methods on molten metal flows [4]. Karimian et al. investigated the influences of the coating thickness on product quality. When the coating film is thin, the amount of pyrolysis gas emitted from the foamed model is higher, and the amount of residue due to pyrolysis is reduced [5]. In addition, studies on the analysis of molten metal flow behavior in vanishing model casting have been actively conducted using CFD simulation [6, 7].

This study proposes a new casting design for the production of large castings by full mold casting. In this method, a residue trap is installed at the product part to prevent the occurrence of residue defects, and the optimal design of the residue trap is realized by using CFD simulation and the shape optimization method. The effectiveness of this method is demonstrated through casting experiments using an actual full mold casting.

2. Parameter identification for CFD simulation

In general castings such as sand casting, molten metal is poured into a hollow mold. In contrast, in full mold casting, molten metal replaces a foam model. Therefore, because the flow of metal differs greatly between full mold casting and normal casting, it is necessary to understand the phenomena that actually occur in the mold.

In full mold casting, the heat of the molten metal decomposes the foam model and generates gaseous pyrolysis products. The thermal decomposition products are successively discharged through the coating mold into the sand mold. If the gas layer of the pyrolysis products is thin, the rate of heat transfer from the molten metal to the foam model will increase, as will the rate of molten metal flow. Conversely, the thicker the gas layer of the pyrolysis products, the lower the heat transfer rate and the lower the flow rate of molten metal. Therefore, the flow metal is determined by the complex interaction of multiple factors such as the metal's temperature, its position in the mold, the material and morphology of the foam model, and the thickness and composition of the coating mold.

In the CFD software used in this study, a foam model is represented as an obstacle that disappears when heated. Therefore, the flow of molten metal is hardly affected by pressure and inertia, but depends on the heat transfer phenomenon. Specifically, the heat transferred from the metal to the foam model at their interface is calculated. Subsequently, depending on the amount of heat, the foaming model disappears and the metal migrates. Therefore, the average inflow velocity U_{front} of

the interface between the molten metal and the foam model can be approximated by the following Equation [8].

$$U_{front} \approx \frac{H_0}{\rho C_p} \qquad (1)$$

where H_0 is the apparent heat transfer coefficient between the metal and the foam model and represents the ease of heat transfer to the foam model. The products of ρ and C_p are the density and specific heat of the foam model.

In the full mold casting, the heat of the metal decomposes the foam model and generates gaseous pyrolysis products. The pyrolysis products are discharged into the sand mold through the coating process. These products are smaller than the metal when the metal is above the foam model. Therefore, the thickness of the gas layer between the metal and the foam model due to the pyrolysis products is reduced. Therefore, the heat transfer rate is expected to be high. On the other hand, when the metal is located below the foaming model, the thickness of the gas layer between the metal and the foaming model is increased and the heat transfer rate is considered to be low. In the CFD simulator used in this study, considering this effect in the gravity direction, the flow rate of metal in the gravity direction is defined by Eqs. (2) and (3) using the parameter E_g [8].

$$U_{flont} \approx \frac{H}{\rho C_p} \qquad (2)$$

$$H = H_0 \cdot \left(1 + E_g \cdot sign(g_n) \cdot \frac{\sqrt{|g_n| \cdot l}}{\sqrt{|g_n| \cdot l} + \frac{H_0}{\rho C_p}} \right) \qquad (3)$$

where g_n is the perpendicular component of the gravitational acceleration to the metal interface and l is the surface roughness of the metal. The product of these
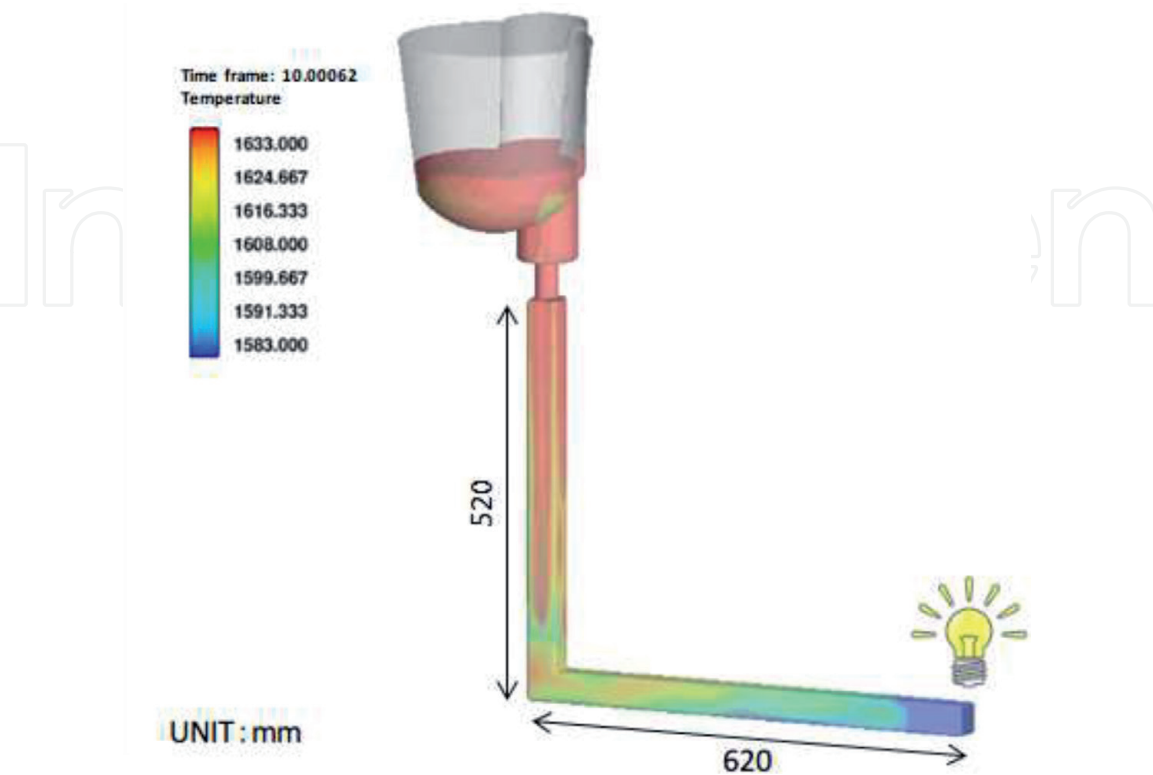

Figure 1.
CFD simulation model for identification experiment.

values expresses the difficulty of heat dissipation of the foam model. Although the model expressed by this equation does not exactly represent the generation of pyrolysis products and the thickness of the gas layer, it is thought that the flow of metal, which is close to the real phenomenon can be expressed by setting appropriate values for each parameter. In this study, casting experiments and molten metal flow analysis were conducted for the model shown in **Figure 1** to obtain the appropriate values of the unknown parameters H_0 and E_g in Eq. (3).

The metal was FC300 gray cast iron, and the pouring temperature was set at 1683 K. Foamed polystyrene with a foaming factor of 60 times was used for the model. A water-based mold coating agent for full-molded cast iron was used for the coating, and the coating film was about 2 mm thick. Silica sand with an AFS grain size index of 36.7 was used as the casting sand. A stopper system was used for pouring the metal. The arrival time of the metal was measured by inserting a touch sensor into the end of the model; this sensor emitted. The experimental results show that the start to the finish of pouring was 7.2 s. The casting weight was 35 kg.

Next, CFD simulations were performed. The parameters in Eq. (3) were set to $\rho = 16.7$ kg/m^3 and Cp = 2100 J/(kg-K). In order to make the arrival time of the metal consistent with that of the experiment and the simulation, the parameter H0 was adjusted based on the definition of Eq. (3), and good results were obtained at H0 = 5500 W/(m2-K) and Eg = 0.5. We therefore use these values in the simulations in this study.

3. CFD analysis and new gating system

3.1 Design of gating system based on CFD analysis

In this study, a capstan drum (**Figure 2**) is used as the product shape. Also, a casting runner with a diameter of 30 mm is used for the solution. The capstan drum was analyzed for metal flow using the two gating systems shown in **Figure 2(a)** and **(b)**.

Gating system A has a gate directly on the arm, which is considered to be prone to many residue defects. Since an enormous amount of time would be required to analyze everything from the pouring to the filling of the product part, a simple
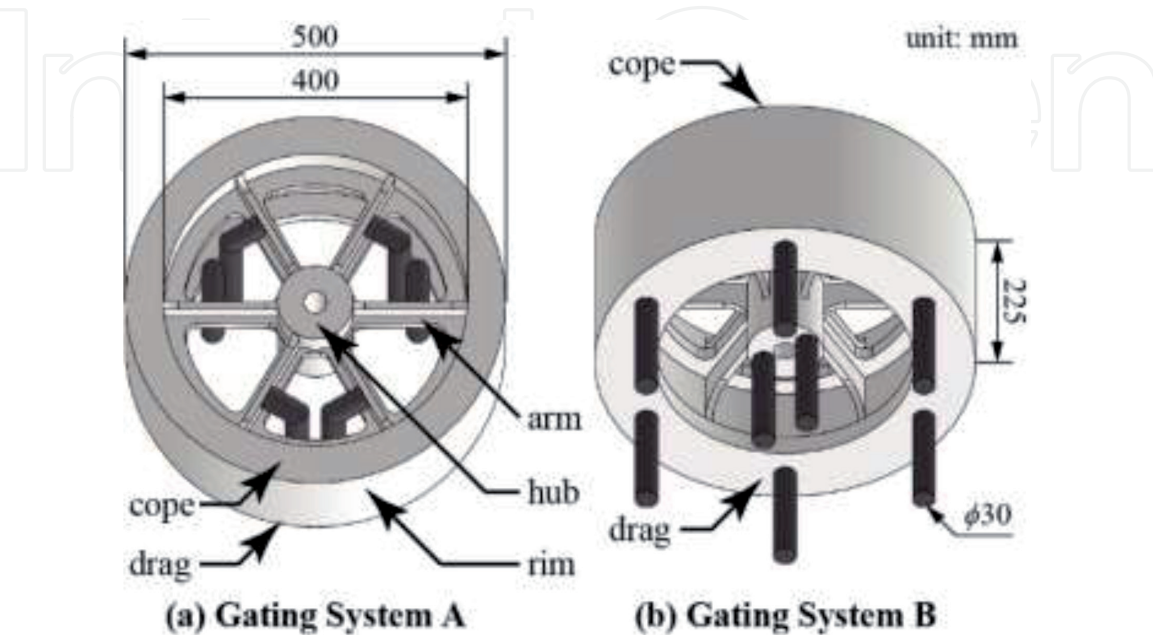

(a) Gating System A   (b) Gating System B

Figure 2.
Shape of capstan drum and gating systems.

model in which metal flows into the product part at a constant pressure from the gate was used. The inflow pressure was set at 1.425×10^5 Pa in absolute pressure, and the temperature of the pouring molten metal was set at 1623 K. The pouring temperature of the metal was set at 1.425×10^5 Pa in absolute pressure. In addition, since the shape was symmetrical, we were able to cut the analysis area in half to reduce the analysis time.

The results of the CFD analysis are shown in **Figure 3(a)**. As shown by the dashed ellipses, the metal flows by gravity from top to bottom. Due to the difference between the density of the metal and the density of the gas and residue generated by the pyrolysis, the metal would entrain the gas and residue, which would affect the occurrence of residue defects.

Then, gating system B is modified to install gates at the rim and hub to improve the flow of gating system A. To prevent the formation of defects in the residue, the pouring temperature was increased by 20 K to 1643 K.

A molten metal flow analysis was performed on the drum using this gating system B. The results of the analysis are shown in **Figure 3(b)**. The flow in the rim proceeds gradually from the bottom to the top, which makes it difficult for the metal to entrain gas and residue. In addition to the increase in temperature, these flows may actually reduce the number of residue defects.

In other words, if a gate is installed on the arm as in gating system A, a drop-in flow occurs, leading to the generation of residue defects, so the gate must be installed on the bottom of the hub and rim as in gating system B. If the
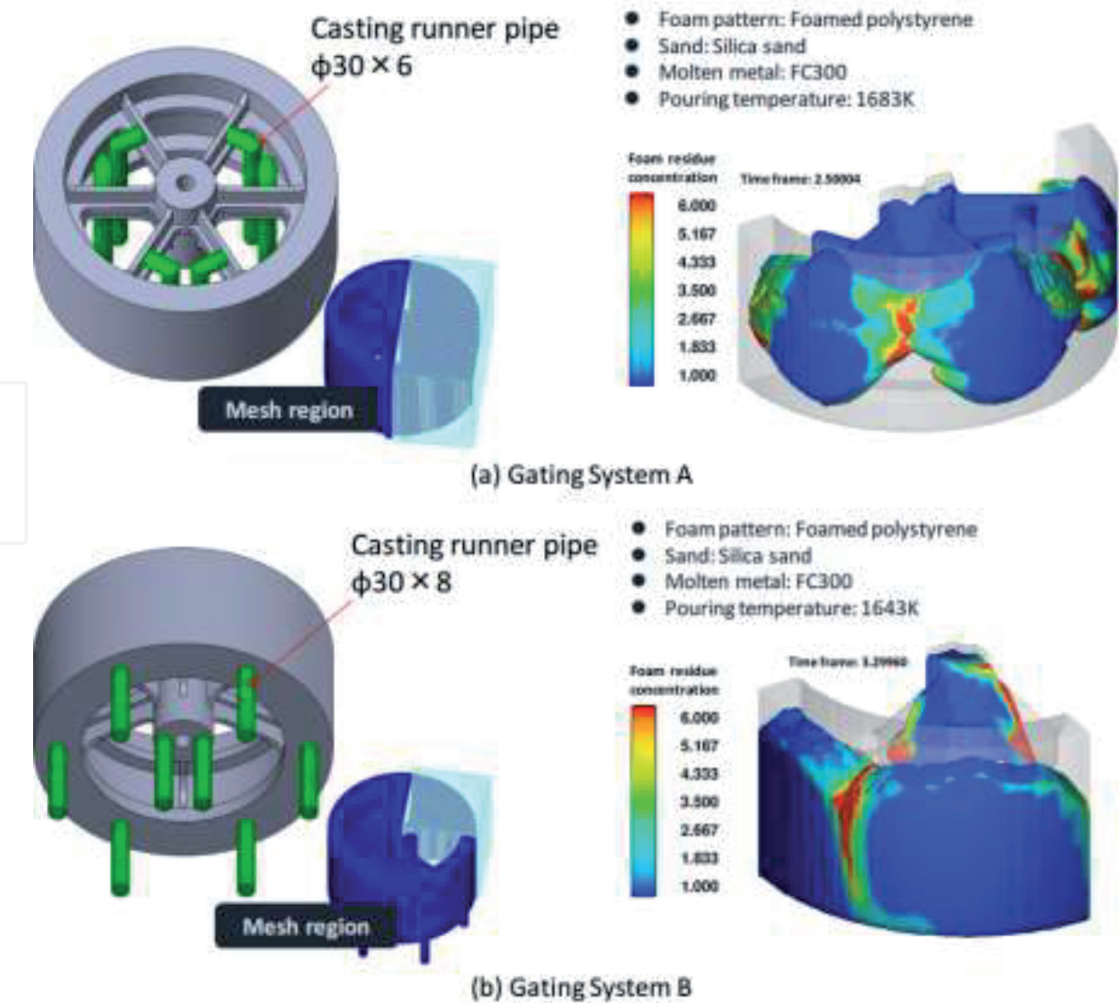

Figure 3.
Results of flow analysis for capstan drum.

pouring temperature is increased to prevent residue defects, the temperature at the completion of filling will also be high, and therefore, to prevent shrinkage defects the pouring temperature should not be increased. Therefore, to prevent both residue defects and the formation of a shrinkage cavity, a new casting plan that allows the suppression of residue defects without increasing the pouring temperature is required.

3.2 New gating system for full mold casting foam residue traps

By installing a gate at the bottom of the rim, the metal cannot avoid merging in the rim. If the pouring temperature cannot be increased, residue defects are more likely to occur. This requires the discharge of metal that contains residue from the rim. Therefore, we propose a new gating system: foam residue traps. For shrinkage nests, this system allows us to lower the temperature of the pouring metal. Although lowering the pouring temperature may increase the number of defects in the residue, a trap is installed on the side of the rim at the position where the metal joins with the metal to collect the residue, and the metal that is free from residue is recovered. This makes it possible to reduce residue defects.

In order to verify the effect of discharging molten metal entrapped by residue traps, a gating system was designed as shown in **Figure 4**. CFD analysis was performed for this. The analysis conditions are the same as in the previous section, except that a residue trap was installed.

The results of the CFD analysis are shown in **Figure 5**. The results of the analysis are velocity vectors of the metal, which are cross-sections based on the center of the height of the capstan drum. Horizontal cross-sections are set at −120 mm, 0 mm, and 120 mm height, respectively. At the 0 mm and 120 mm cross-sections, there is a vector of the flow from the inside of the residue trap to the rim. Therefore, metal that is entrapped in the residue may flow into the rim. Since the interface between the foam model and the metal is filled with molten metal with resistance due to combustion, it is considered that convection is formed by a flow that has no place to go. Therefore, it is necessary to design an appropriate casting plan to prevent the backflow of metal to the rim side due to convection inside the residue trap.
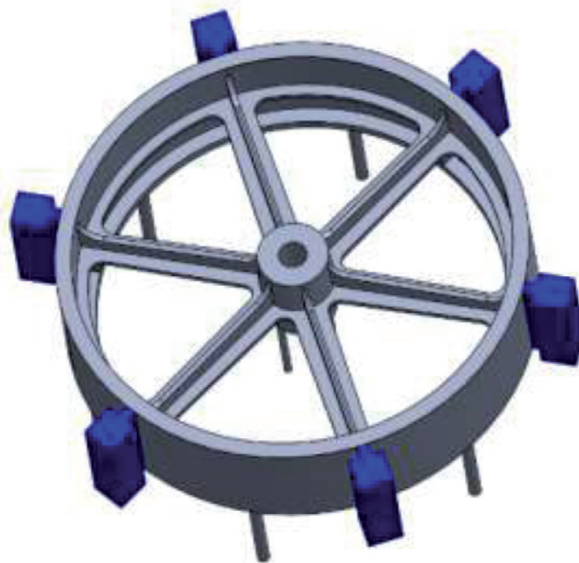

Figure 4.
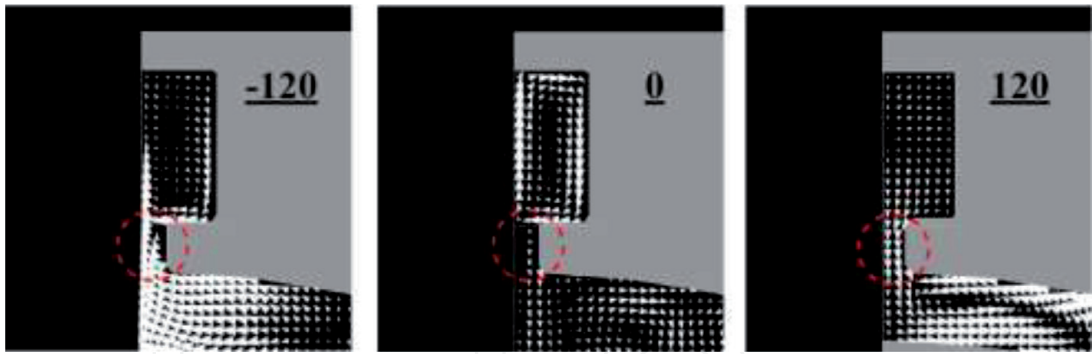*Capstan drum with traps for preventing foam residues.*

Figure 5.
The velocity vectors on the horizontal sections for the foam residue trap.

3.3 Optimal design of residue traps

Based on the results of the analysis in the previous section, the bottom of the rim is considered the best location for the gate, but in any case, residue defects will be generated by molten metal joining in the rim. In this study, a residue trap is proposed as a gating system for collecting molten metal that can join together and directly collect metal that is entrained with residue, and a new casting method for large castings is presented.

The optimal design of the residue trap is used for the capstan drum shown in **Figure 2**. In optimization, the dimensions defined as design variables are varied within a set range to find the optimal combination. This combination increases with the number of design variables, and the time required for optimization becomes enormous. Therefore, the number of design variables must be set to the minimum necessary.

The basic shape of the residue trap and the locations where the design variables were set are shown in **Figure 6**. The design variables were defined with five variables, x_1 to x_5. Six of these residue traps are installed evenly across the sides of the rim and are interlocked depending on the value of the design variables, all of which have the same shape.
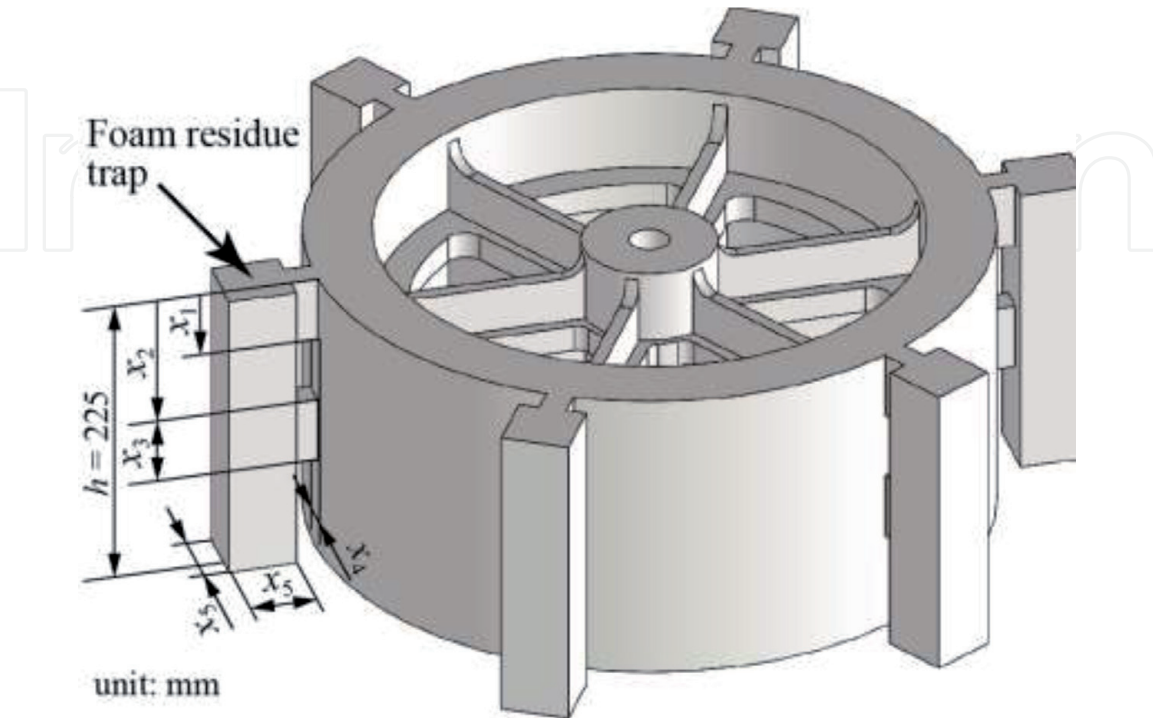

Figure 6.
Foam residue traps of capstan drum and design variables.

Three objective functions are defined as evaluation indices for optimization. The first objective function, J_1, is an indicator of the amount of residue in the rim. The residue in this CFD software is defined as the diffusion of the transport equation equal to the volume of the foam model replaced by metal. This amount of residue can actually be calculated as the residue volume fraction a_k for each calculated cell k, which represents the volume fraction of the residue contained in the cell in terms of solid time equivalent, and J_1 is defined as the following equation, where J_1 is this residue volume fraction averaged for each cell in the rim.

$$J_1 = \frac{\sum_{k=1}^{n} a_k}{n} \tag{4}$$

where n is the number of cells in the rim. In other words, J_1 represents the volume fraction of the residue in the entire rim. The smaller the value of J_1, the lower the residue defects are expected to be in the actual castings. In this capstan drum simulation, the number of cells in the rim is $n = 32575$, where each side is a cube of 5 mm.

The second objective function, J_2, is defined as the contact area between the rim and the residue trap. J_2 is calculated using the design variables x_1, x_3, and x_4 by the following equation.

$$J_2 = x_1 x_4 + x_3 x_4 \tag{5}$$

The smaller the value of J_2, the easier it is to remove the residue traps and the better the shape.

The third objective function, J_3, is defined as the volume of the residue trap itself, which is calculated using the design variable x_5 and the height of the residue trap, h, as follows.

$$J_3 = x_5^2 h \tag{6}$$

The smaller the value of J_3, the higher the material yield and the better the gating system.

Based on these definitions, we added geometric constraints and finally formulated this optimization problem.

$$\begin{aligned}
\textit{Minimize } & J_1(x_1,,\ldots,,x_5), J_2(x_1,,x_3,,x_4), J_3(x_5) \\
\text{Subject to } & 0\,mm \leq x_1 \leq x_2 \leq 225\,mm \\
& 0\,mm \leq x_2 + x_3 \leq 225\,mm \\
& 10\,mm \leq x_4 \leq 30\,mm \\
& 30\,mm \leq x_5 \leq 120\,mm
\end{aligned} \tag{7}$$

We applied NSGA-II [9], a multi-objective genetic algorithm, to this optimization problem. The algorithm was set up with 50 individuals per generation, congestion tournament selection as the selection method, and BLX-α as the mating method. We also decided to terminate the optimization when the percentage of individuals generated more than 2 generations ago in the population of the focused generation exceeded 70%, or when the number of generations reached 30.

The distribution of all the individuals generated by the optimization for the objective function values is shown in **Figure** 7.

The total number of individuals generated was 775. This figure shows that the volume fraction of residue J_1 and the volume of residue trap J_3 are in a trade-off relationship with each other. C in the figure shows the objective function values of

the residue traps in which no residue defects occurred in the preliminary experiments. Therefore, in this optimization we selected the individual that is superior for both objective functions as the optimal solution for this C. The final optimal shape is shown in **Figure 8**. The values of the design variables of the optimal solution are shown in **Table 1** and those of the objective function are shown in **Table 2**.
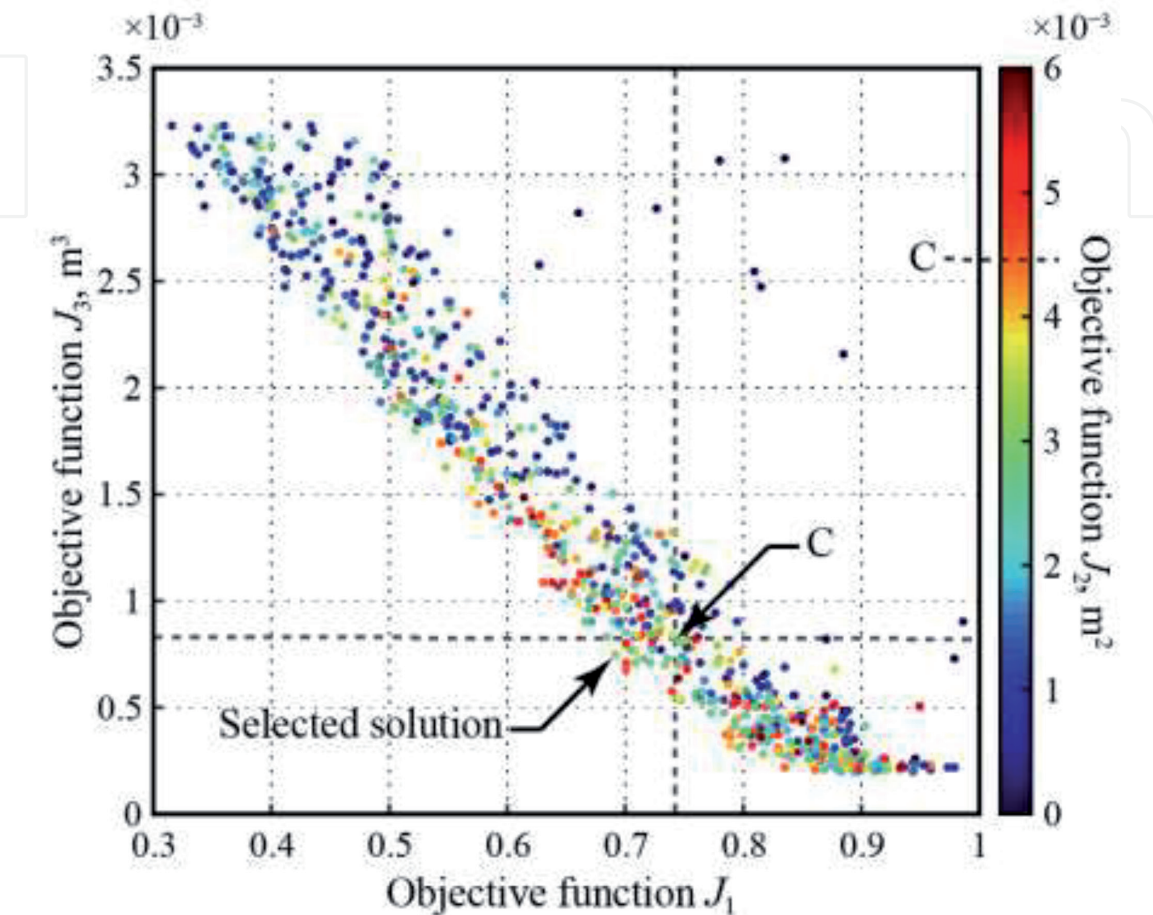

Figure 7.
Distribution of all analyzed individuals in optimization.

(a)   **(b)**
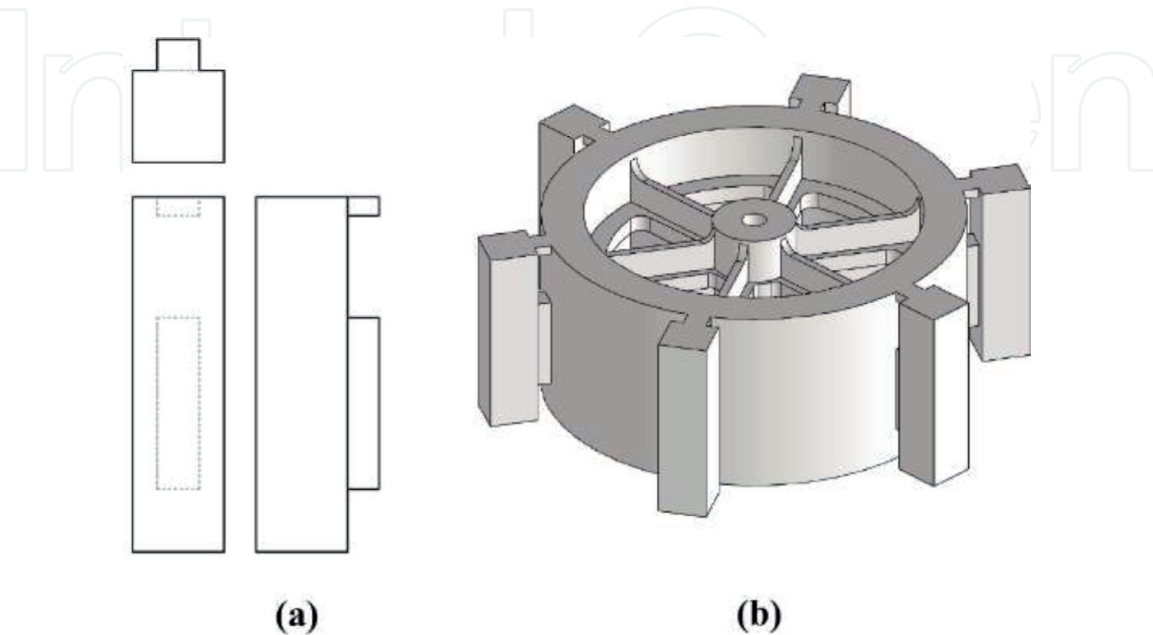
Figure 8.
Optimized shape of foam residue trap. (a) Foam residue trap. (b) Whole shape of casting.

x_1 [mm]	x_2 [mm]	x_3 [mm]	x_4 [mm]	x_5 [mm]
11.58	76.50	108.82	27.05	57.57

Table 1.
Values of design variables for optimal solution.

J_1 [−]	J_2 [m²]	J_3 [m³]
6.906×10^{-1}	3.257×10^{-3}	7.456×10^{-4}

Table 2.
Values of objective functions for optimal solution.
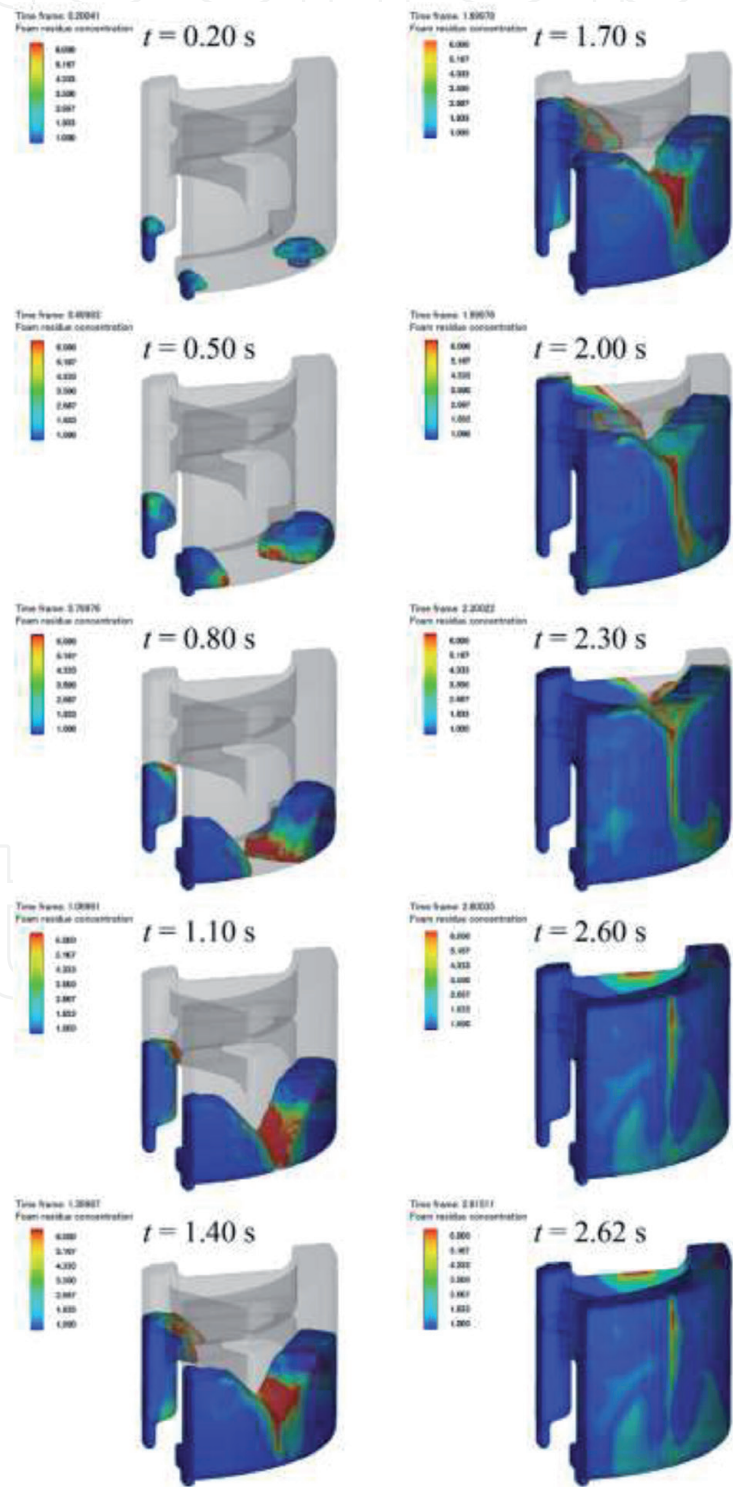
Figure 9.
Fluid behavior without foam residue trap.
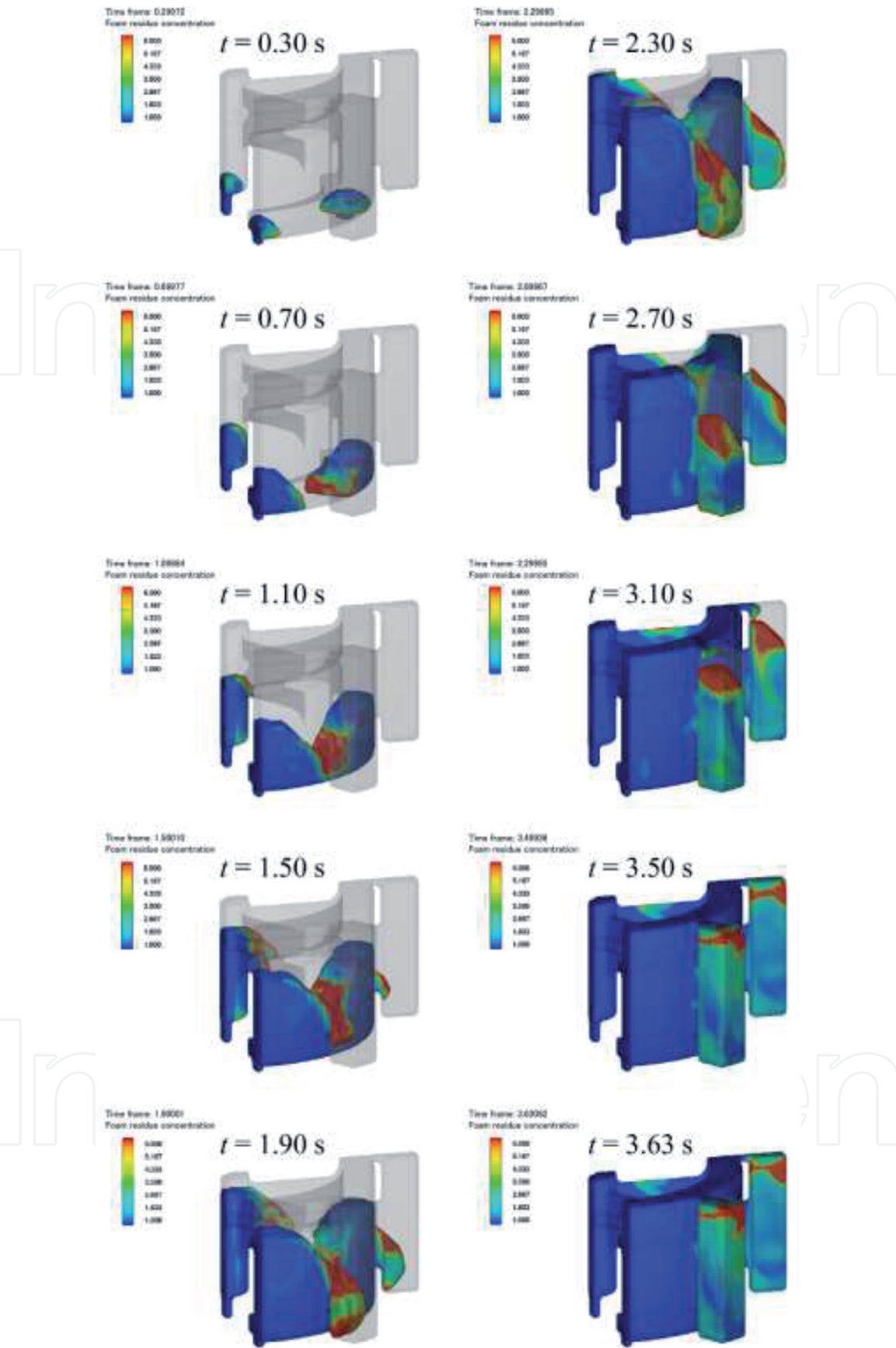
Figure 10.
Fluid behavior with shape-optimized foam residue trap.

In order to verify the effectiveness of the optimal shape, CFD analysis was performed and compared between the conventional method without a residue trap and the residue trap method with the optimal shape. The flows for the conventional and residue-trapping methods are shown in **Figures 9** and **10**, respectively.

In the conventional gating system, the metal flow shows that the residue is spreading inside the rim, and it is thought that the following factors influence the development of residue defects. The volume fraction of the residue in this case was $J_1 = 1.013$. On the other hand, the residue trapping method has an opening in the residue trap where the metal containing residue agglomerates, through which residue is effectively collected into the trap. The part of the rim that is not in contact with the residue trap suppresses the backflow of metal containing residue. Due to these effects, the optimal shape of the residue trap is efficient for collecting residue and effective for capturing residue. The volume fraction of residue is 0.6906, which is more than 30% lower than that of the conventional method.

4. Verification of effectiveness by casting experiments

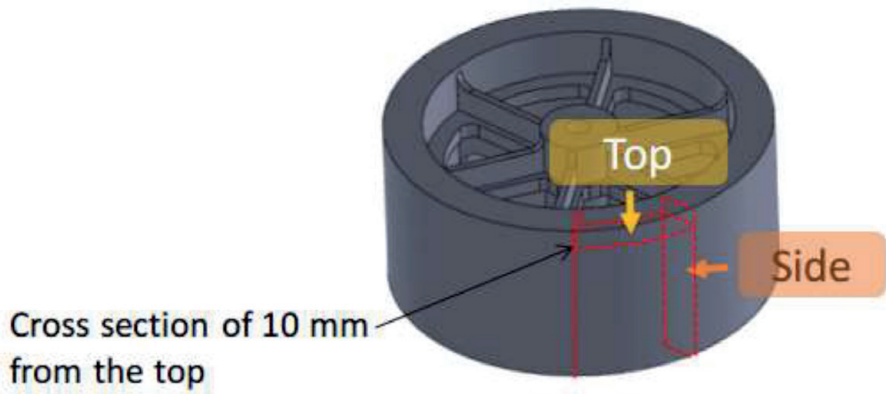Casting experiments were conducted to verify the effectiveness of the optimally designed residue trap.

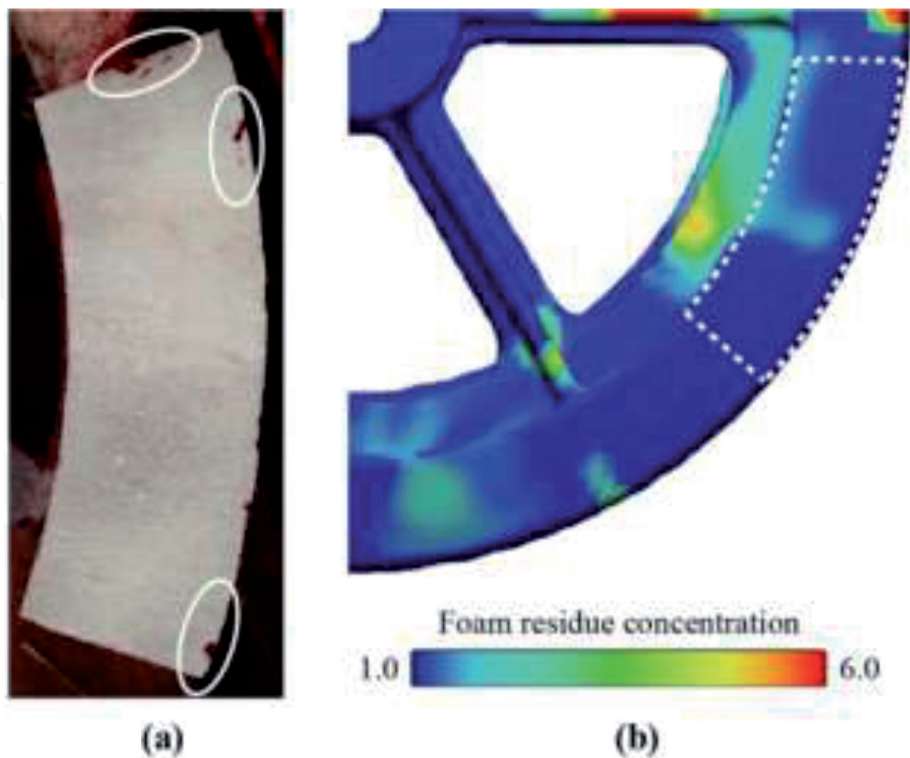**Figure 11.**
Cross section of capstan drum for experiments.

Figure 12.
Evaluation of foam residue defect for casting without foam residue trap. (a) Experimental result. (b) Flow analysis result.
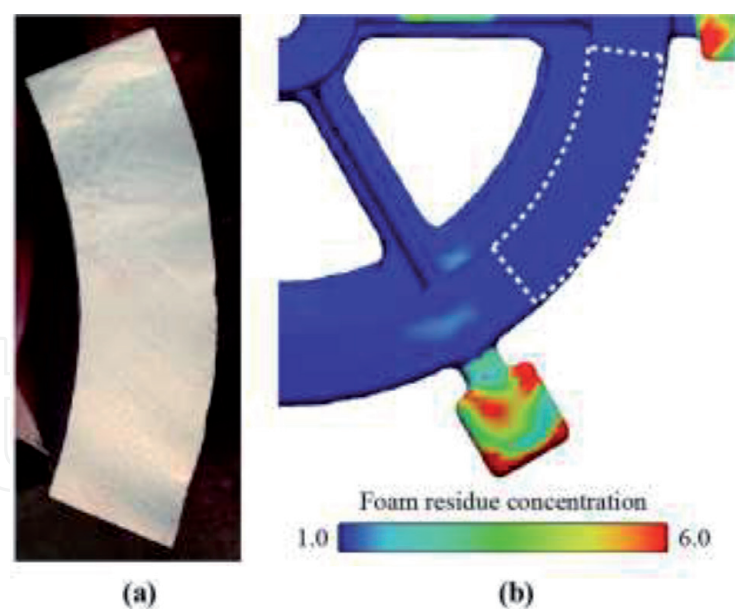
Figure 13.
Evaluation of foam residue defect for casting with shape-optimized foam residue trap. (a) Experimental result. (b) Flow analysis.
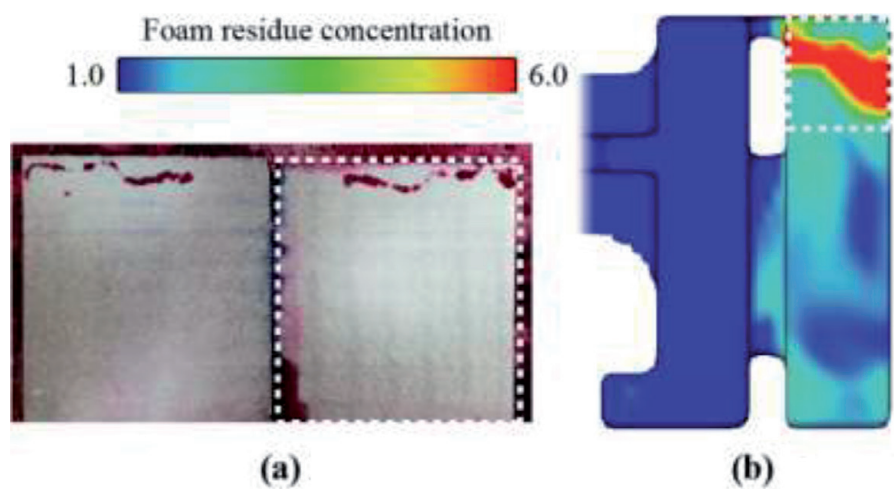

Figure 14.
Evaluation of foam residue defect in foam residue trap. (a) Experimental result. (b) Flow analysis result.

In this study, two types of capstan drums were cast: one with a conventional method without a residue trap and the other with an optimized residue trap method. The temperature of the metal was set to 1623 K, and the other conditions were the same as in the experiments in Section 2. After casting and cooling, the product was cut to make a test specimen, and the cut surface was color-checked to compare the defects. As shown in **Figure 11**, the position where the product part was cut was set to a horizontal plane 10 mm downward from the top of the rim because the residue tends to accumulate on the top of the rim.

The experimental results of the conventional plan and the corresponding simulation results are shown in **Figure 12**. This result suggests that this was caused by the residue of the foam model generated during the filling of the molten metal and remaining in the rim of the drum. The simulation results in **Figure 12(b)** indicate that residue defects are more likely to occur around the specimen, although the simulation does not fully predict the distribution of residue.

Figure 13 shows the experimental results of a residue trapping method using the optimal shape and the corresponding simulation results.

Slight shrinkage nests were observed in the specimens, but no residue defects were observed. Similarly, in the simulation results, there was almost no residue around the specimen. Therefore, the residue traps were also cut in the same way as the test specimens, and the color inside each trap was checked. The results and the corresponding simulation results are shown in **Figure 14**. Residue defects were observed in the residue trap, indicating that the residue generated inside the product was captured well by the trap. Therefore, this study confirms that the residue trapping method using the optimal shape effectively reduces residue defects.

5. Conclusion

In this study, a new residue trapping method is proposed to suppress defective residues, which are a problem in manufacturing large castings by the full mold casting method. To maximize the performance of the residue trap, the shape of the trap was optimized by using CFD simulation. The effectiveness of the optimized residue traps was verified by casting experiments, which showed that the effectiveness of the optimized traps can reduce residue defects better than those without traps.

Author details

Yuto Takagi, Masahiro Inagaki and Ken'ichi Yano*
Mie University, Mie, Japan

*Address all correspondence to: yanolab@robot.mach.mie-u.ac.jp

IntechOpen

References

[1] J. Thiel and S. Ravi: Analysis and Prediction of Casting Defects Using Casting Simulation. Proc. 71st World Foundry Congress, Bilbao (WFO) (2014)

[2] K. Kanazawa, K. Yano, J. Ogura, and S. Baba: New Curve Optimization Method and Its Application to Shape Design for Die Casting Using a CFD Simulation. No. 62541 in Proc. ASME 2013 IMECE (2013)

[3] T. Maruyama, N. Goto and T. Kobayashi: Thermal decomposition products of expanded polystyrene pattern in evaporative pattern casting of cast iron. Journal of Japan Foundry Engineering Society. 2009;81(3):117-122

[4] S. Koroyasu and M. Matsuda: Effects of high insulating coat on cooling rate of aluminum alloy in evaporative pattern casting process. Journal of Japan Foundry Engineering Society. 2004;76(8):678-686

[5] M. Karimian, A. Ourdjini, M. Hasbullah and H. Jafari: Effect of pattern coating thick-ness on characteristics of lost foam Al-Si-Cu alloy casting. Transactions of Nonferrous Metals Society of China. 2012;22(9):2092-2097

[6] C. W. Hirt and M. R. Barkhudarov: Modeling the Lost Foam Process with Defect Prediction. Flow Science Tech. Note. 1997;FSI-97-TN45

[7] C. W. Hirt and M. R. Barkhudarov: Predicting Defects in Lost Foam Castings. Modern Casting (2002)

[8] C. W. Hirt: Modeling the Lost Foam Process with Defect Predictions Progress Report: Lost Foam Model Extensions, Wicking. Flow Science Tech. Note. 1999;FSI-03-TN45-1

[9] K. Deb, A. Pratap, S. Agarwal and T. Meyarivan: A Fast and Elitist Multiobjective Genetic Algorithm: NSGA-II. IEEE Transactions on Evolutionary Computation. 2002;6(2):182-196